Dissolved Rare Earth Elements in the central-western sector of the Ross Sea, Southern Ocean: geochemical tracing of seawater masses

Clara Turetta[a*], Elena Barbaro[a,b], Gabriele Capodaglio[a,b], Carlo Barbante[a,b]

[a]Institute for the Dynamics of Environmental Processes-CNR, Dorsoduro 2137, 30123 Venice, Italy;

[b]Department of Environmental Sciences, Informatics and Statistics - University Ca' Foscari, Dorsoduro 2137, 30123 Venice, Italy

Corresponding author: *clara.turetta@idpa.cnr.it, Institute for the Dynamics of Environmental Processes-CNR, Dorsoduro 2137, 30123 Venice, Italy, ph. +390412348947.

Other authors e-mail: barbaro@unive.it, capoda@unive.it, barbante@unive.it

Dissolved Rare Earth Elements in the central-western sector of the Ross Sea, Southern Ocean: geochemical tracer of seawater masses

Clara Turetta[a*], Elena Barbaro[a,b], Gabriele Capodaglio[a,b], Carlo Barbante[a,b]

[a]Institute for the Dynamics of Environmental Processes-CNR, Dorsoduro 2137, 30123 Venice, Italy;

[b]Department of Environmental Sciences, Informatics and Statistics - University Ca' Foscari, Dorsoduro 2137, 30123 Venice, Italy

Abstract

Also if several data focussed on rare earth elements (REEs) in southern hemisphere were published we present here the first data, at our knowledge, on vertical profiles of dissolved REEs from 71 samples collected in the central-western sector of the Ross Sea (Southern Ocean). REEs have been measured in the water masses collected in the Ross Sea during the 2002-2003 and 2005-2006 austral summer. Also 4 samples collected during a test experiment, as part of WISSARD Project (Whillans Ice Stream Subglacial Access Research Drilling), beneath the McMurdo Ice Shelf were analysed. Results show significant differences in the REE pattern of main water masses present in the Southern Ocean, in particular we can observe some signature in the High Salinity Shelf Water (HSSW), Ice Shelf Water (ISW), low Salinity Shelf Water (LSSW) and Modified Circumpolar Deep Water (MCDW).

A significant increase in Terbium (Tb) concentration is observed in the HSSW, ISW, which are the principal water masses contributing to the formation of Antarctic Bottom Water (AABW) in the Ross Sea area, and LSSW. Part of the HSSW samples also show an enrichment in the neodymium content. Therefore the dissolved REE composition could be used like tracers in the understanding the deep circulation of the Pacific sector of the Southern Ocean.

We hypothesise that the characteristic dissolved REE pattern may derive from the composition of source area of crustal inputs and/or from the hydrothermal activity of the central-western area of the Ross Sea.

We can also hypothesise that the Tb anomaly observed in the AABW on the south Australian platform of the Southern Ocean could be partially explained by the contribution of AABW generated in the Ross Sea region.

1. Introduction

The Ross Sea is a key area for the formation of new waters and plays an important role in the ventilation of world ocean bottom waters. It is defined as the waters over the continental shelf limited to north by the ideal line between Cape Colbeck and Cape Adare and to south by the Ross Ice Shelf (RIS) (Dinniman et al., 2003; Cincinelli et al., 2008). The only one water of external origin influencing the Ross Sea mass waters is the Circumpolar Deep Water (CDW), a warm, nutrient-rich and salty water carried around the Antarctica by the Antarctic Circumpolar Current (ACC) (Catalano et al., 2000; Orsi and Wiederwohl, 2009). Its mixing with surface and

shelf waters of the Ross Sea generates the so-called MCDW. The most characteristic water of the Ross Sea is the HSSW, that flowing beneath the RIS contributes to formation of ISW. The knowledge of the trace element distributions in the waters of the Ross Sea is partial and primarily related to certain elements such as heavy metals (Fe, Cd, Cu, Pb, Mn, Zn, etc.) (Capodaglio et al., 1989; Gragnani and Torcini, 1992; Abollino et al., 1995; Scarponi et al., 1995; Scarponi et al., 1997; Capodaglio et al., 1998; Fitzwater et al., 2000; Frache et al., 2001; Grotti et al., 2001; Coale et al., 2005; Corami et al., 2005; Turetta et al., 2010; Rivaro et al., 2011).

Trace elements distribution in Ocean waters are controlled by two principal factors, origin and processes affecting the dissolved/particulate partition; therefore their vertical concentration assume characteristic profiles related to their origin and geochemical reactivity (Bruland, 1983). There are also evidence that interaction with dissolved organic matter play an important role in the distribution also of reactive elements not involved with biological cycles as well lead (Capodaglio et al., 1990). The complexity of cycles controlling the trace elements distribution make quite difficult to define level of concentration in specific water masses, on the other hand elemental composition could be a good identifier of specific water masses. Therefore is particular important to identify markers of specific water masses to follow their contribution to the general oceanic circulation.

REEs have a lithogenic origin (Goldstein and Hemming, 2003) in the ocean with contributions from aerosol particles and dissolved rivers loads (Sholkovitz et al., 1999; Dubinin, 2004). Other studies suggest that the dominant source of REE in ocean is the dissolution of sediments from continental shelves (Zhang et al., 2008) while in ice-covered oceans the major source of REEs probably is particulate matter rafted by sea ice and glacial ice (Winter et al., 1997). Due to their coherence in terms of geochemical behaviour the REEs may be a useful tool to trace the different seawater masses and to recognize their provenance and their fate; because of their relatively short mean oceanic residence time REEs can be useful for

characterising water masses from the point of view of ocean circulation and geochemical behavior (Piepgras and Jacobsen, 1992; Byrne and Sholkovitz, 1996; Alibo and Nozaki, 2004). In particular, as reported by Nozaki and Alibo, "the vertical profiles of light REEs (LREEs) and some medium REEs (MREEs) are variable from basin to basin" and "the heavy REEs (HREEs) are largely governed by the horizontal processes of ocean circulation" (Nozaki and Alibo, 2003).

The Southern Ocean is considered one of the most important feeders of world bottom waters. By comparing our data with literature ones we may hypothesize the contribution of new formation waters of Ross Sea to water masses of South Pacific Ocean. Taking in account the behaviour of terbium (Tb) and neodymium (Nd) in the new waters HSSW, ISW, LSSW, and also in MCDW we can characterize the AABW generated from the Ross Sea new waters (Orsi et al., 1999; Corami et al., 2005; Orsi and Wiederwohl, 2009) and recognize this water mass in the south Australian platform. With this purpose we have normalized REE concentrations against the North Pacific Deep Water (NPDW) composition (Nozaki, 2001).

The aim of this paper is to propose a new data set of dissolved REEs from the Ross Sea, Southern Ocean, to contribute to the knowledge of inter-basin circulation on the basis of the REE pattern as tracer of seawater masses and to recognize possible sources of REE in Ross Sea water. Total dissolved REE concentrations were measured along the vertical profile at various sites in the Ross Sea (Antarctica) in order to emphasize characteristic anomalies of water masses contributing at the formation of AABW.

2. Methodology and characteristics of research area

2.1 Material and methods

Within the framework of the Italian expeditions in Antarctica on board the R.V. Italica, during the austral summer 2002–2003 and 2005-2006, 71 seawater samples from 10 depth

profiles were collected in the western sector of the Ross Sea (Southern Ocean, Antarctica). Figure 1 shows the location of sampling sites while table 1 resume the spatial coordinates of each profiles, maximum depth and the year of campaign; the sites were chosen in order to evaluate some of relevant water masses present in this area. The sampling strategy was driven on the basis of the in situ measurements of salinity, temperature and dissolved oxygen along the water column (we decide where to close the 20 L Go-Flo bottles and collect samples with the aim to have all the waters with different characteristics in the studied profile). After sampling, the hydrological bottles were immediately transferred into a mobile clean-laboratory (Class 100) installed on board, the samples were filtered and immediately frozen at -20°C for transport to Italy without any additional treatment. Sampling strategy, shipboard filtration and storage, sample handling and analysis procedure were described in previous papers (Turetta et al., 2004; Turetta et al., 2010).

Details for samples from WISSARD project are reported in Field Report 2012 (The Wissard Science Team, 2012); briefly, 4 samples were collected (latitude 77°53.25' S longitude 167° 0.30' E) using both go-flo and niskin bottles under a significant thickness of ice shelf (56 m), and water depth (917 meters below sea level), transported back to Crary Lab at McMurdo Station for freezing and storage and then shipped frozen to Italy. Sample handling and analytical procedures were the same used for oceanographic campaign samples and described in previous papers as reported above.

Analyses were carried out using a Sector Field Inductively Coupled Plasma- Mass Spectrometer (SF-ICP-MS, Element2 Finnigan-MAT, Bremen, Germany), coupled with a desolvation unit (Aridus, Cetac Technologies, Omaha, NE, USA), on diluted samples (1:10 with ultrapure water, Pure Lab Ultra Water System-Elga Lab Water, High Wycombe, UK) acidified with ultrapure nitric acid (1:10 v:v, Romil®UPA, Cambridge, UK). Before each analysis session

sensitivity, stability and oxide formation were carefully checked analysing a diluted seawater sample spiked with 100 ng L^{-1} of Rh and Ce.

The quantification of REEs was carried out by a matched calibration method. Six aliquots of one sample were spiked with a multi-element standard solution (0, 0.2, 0.5, 1, 2, 5,10, 20 and 50 pg mL–1, from a 1000 mg L^{-1} ICP-MS stock solution-Spex-CertiPrep, Metuchen, NJ—USA). Although there is not certified values for REEs in CRM-NASS5-NRCC (Seawater Certified Reference Material for Trace Elements from National Research Council of Canada) we have chosen to use this certified reference materials due to the information values from literature (Willie and Sturgeon, 2001; Kajiya et al., 2004; Lawrence and Kamber, 2007) and from Geological and Environmental Reference Materials web-site (GeoReM, http://georem.mpch-mainz.gwdg.de/) to verify the accuracy of our measurements (table 2).

Tests on "blank solutions" (ultrapure water, HNO_3 1:10 v:v and internal standard at 1 ng mL^{-1} concentration; Scandium and Rhodium were used as internal standards) were performed in each analytical session before analysis of the seawater samples to carefully consider the effects of dilution, acidification and internal standard addition; no significant signal was observed compared to expected values for real samples (Turetta et al., 2004).

The results (mean and standard deviation) of the analyses performed on ten blank solutions are reported in table 2. Detection limits were calculated as two times the standard deviation of the blank solution signal to evaluate the relevance of our measurements (Thompson et al., 2002). Possible interferences were accurately considered in a previous paper (Gabrielli et al., 2006).

2.2 Hydrology of research area, physical characteristics of the water column and bottom topography of the Ross Sea

The Southern Ocean is a key region to understand the variation of the global climate and the Ross Sea plays an important role on its circulation. During the austral summer different water masses can be recognised in the Ross Sea: AASW (Antarctic Surface Water), MCDW, HSSW, ISW and LSSW (Jacobs and Giulivi, 1999; Gordon et al., 2000; Holland et al., 2003; Corami et al., 2005). A detailed description of the general characteristics and of potential temperature, oxygen, salinity and fluorescence of the single water masses recognised in the studied area and of the sampling sites are detailed reported in a previous paper (Turetta et al., 2010). Briefly, we report here the principal characteristics of HSSW and ISW, the two masses of new formation of the Ross Sea, and of MCDW. HSSW is identified by a salinity >34.62‰ (Orsi and Wiederwohl, 2009) and a temperature at the sea surface freezing point (−1.89 to −1.8 °C). During the Antarctic summer it is the dominant water in the subsurface of the western sector. It is a dense water mass flowing northward along the Drygalski and Joides Basins till downward to ocean floor re-oxygenating the bottom water. ISW takes its origin from the part of HSSW that moves southward and flows under the Ross Ice Shelf (RIS) (Gordon et al., 2000; Budillon et al., 2002; Holland et al., 2003) and is characterised by a temperature below the sea surface freezing point. It is recognised in the west - central sector, where it comes out from the RIS (Dinniman et al., 2003). While ISW is formed along the RIS, HSSW is formed in the large Ross Sea polynia, an area of open water surrounded by sea ice, and in the small, persistent one close to the Victoria Land coast. Last, MCDW derives from the mixing of CDW with shelf waters (Budillon et al., 2002); it is referred to as the Warm Core of the Ross Sea (Jacobs and Giulivi, 1999) and is characterized by a temperature between +1.0 and −1.5 °C (Dinniman et al., 2003).

The bottom topography of the Ross Sea is quite peculiar, characterized by several pronounced bathymetric highs and lows; the bathymetry of the ridges and swells varies

between 400–600 m showing a general northeast–southwest trend (Karner et al., 2005). The lows and the basins result from scars modelled by glacial erosion induced by ice sheet advances (DeMaster et al., 1996).

Mantyla and Reid hypothesised that Ross Sea waters may contribute to the composition of deep and bottom water in the eastern Indian Ocean (Mantyla and Reid, 1995). The bottom waters coming from Ross Sea to Cape Adare zone collapse along the continental slope proceeding westward and possibly pouring in the abyssal plain of the Australian-Antarctic Basin (Orsi et al., 1999; Orsi and Wiederwohl, 2009). Another way for Ross Sea waters to reach the oceanic floor is represented by the Glomar Challenger Trough; this area represent a major pathway for the export of the super-cooled low-salinity ISW that takes origin under the Ross Ice Shelf (Gouretski, 1999; Gordon et al., 2009).

3. Results and discussion

The samples distribution in the Potential Temperature-Salinity (θ-S) space is shown in figure 2, concentration of REE along the vertical profiles are showed in figs. 3 and 4 while the pattern of the dissolved REEs, as REEs/NDPW ratio (calculated as the ratio between each REE in our samples and each REE in NPDW using data from (Nozaki, 2001) to compare our data with literature ones), in the different water masses is shown in figure 5. The NPDW normalization can help us to identify REEs fractionation "in the dissolved end product in the route of the global ocean circulation" (Nozaki, 2001). We also report as comparison result of the analysis of few samples coming from WISSARD sampling campaign 2012. These samples were collected beneath the RIS, at a depth of c.a. 900 m, South-East of McMurdo station in the framework of first WISSARD campaign (for further details on WISSARD's goals see project web site http://www.wissard.org/).

The concentration of dissolved REEs is in general agreement with value reported in literature (German et al., 1995; Nozaki and Alibo, 2003); only some elements are meanly slightly higher than literature data. We report in table 3 mean, minimum and maximum values for measured REEs and in tables 4 a and b values for ΣLREE, ΣMREE, ΣHREE, La/Yb and Gd/Yb PAAS normalized ratio of each samples as representative of ratio between LREE/HREE and MREE/HREE respectively.

The fractionation that typically occurs in seawater, with a general resulting impoverishment of light REE (LREE) compared to heavy (HREE), in the case of waters of new-formation (ISW and HSSW, in particular) is not clearly evident, although still present (to better highlight this characteristic in figure 6 the relative REEs concentration normalized to PAAS – Post Archean Australian Shale is reported; data from (Lerche and Nozaki, 1998) were used to calculate REEs/PAAS ratio; in table 4 a and b La/Yb and Gd/Yb PAAS normalized ratio are reported); in consideration of difference in the pattern it seems that what most define REEs concentration in these waters are two factors: source area (ice shelf and tongues included) and mixing with other water masses.

To follow the route of water masses in global circulation in Fig. 5 a-g the pattern of REEs normalized respect to NPDW and subdivided for typology of water masses are reported (grouping of different waters was done on the base of θ-S graph). Some peculiarities that characterize and distinguish the different kinds of water identified in the Ross Sea are present but it is also evident that there is a mixing between different waters that results in mixed pattern for various samples especially for those that are in particular areas like sites B, CA3, CA4, CI, and G where new waters meet old water (MCDW).

The new-formation waters appear to be characterized by positive peaks of some elements. The ISW is characterized by a significant peak of Tb, which is recognizable also in LSSW and,

with decreasing intensity, in HSSW and waters deriving from all these, in particular in AABW. In addition, the signal of terbium appears to be more pronounced in the samples of the 2005-2006 campaign compared to those of the 2002-2003 campaign and, for the same type of water mass, in the samples from the sites closest to the RIS (A and F) compared to those from the more external sites (B and H). In order to emphasize different pattern in the REEs distribution a principal component analysis (PCA) was carried out . In figure 7 a-b we report the bi-plots of first component vs second and third component respectively.

The bi-plot let us to summarize in a single graph the sample distributions and the variables (element and physical parameters) that cause this distribution. We have limited our statistical analysis to samples deeper than 200 m to better highlight the distribution of new formation waters. In figure 7a we can observe a clear separation between samples representative of new formation waters (namely HSSW, ISW, LSSW, AASW and AABW) and "old" water (MCDW), represented by samples in the bottom part of graph (red area). In the top part of the same graph that represents the different new waters the differences between HSSW waters already observed in the pattern graphs (figures 5 and 6) are clearly highlighted. In the central part (light green area) we recognize samples collected near the Drygalsky ice tongue and samples connected to this area (samples from profile G and B) while in the top part (green area) there are samples more directly connected to RIS. This separation is principally due to Tb and oxygen from one side and Nd and temperature from the other one. Between these two HSSW areas we also recognize two additional smaller areas that group AABW and ISW samples respectively.

Separation of HSSW samples collected near the Drygalsky ice tongue is well highlighted by third component (figure 7b) that separate these samples from all others. Separation is due to salinity and Nd as already highlighted in figures 5 and 6) but also to Er that seems to well differentiate samples of D profile from all others also if in pattern profile Er peak is not so evident with respect to Nd. The fourth component of PCA, not reported as bi-plot, accounts for

9.30% of total explained variance. It is characterized by salinity and oxygen from one side and temperature from the other scaling samples on the base of these parameters. Because REEs are not relevant in this fourth component it isn't discussed.

Indeed on the base of literature data (Jacobs et al., 2002; Boyer et al., 2005; Orsi and Wiederwohl, 2009) on the freshening of the ocean waters (and of the Ross Sea in particular as result of the increased melting of the RIS) and our results, we can hypothesize that the increased melting of the RIS, with the consequent release of the particulates included therein and fresh water both from shelf itself and subglacial hydrological systems, is the cause or one of the causes of the pattern of REE in the various water masses of new-formation. The increase in the Tb concentration own is in the waters next to the RIS and under the RIS. This hypothesis should be confirmed by analysis of samples coming from the catchment area of the RIS, however the exact provenance of the particulate is outside of the pourpose of this paper.

It should also be noted that HSSW can be differentiate in two subgroups (Figure 5 b-c) with partially different characteristics: the first group of HSSW, which includes samples coming mainly from the sites A and F, is characterized by a very clear peak of Tb, although less pronounced than in the ISW. The second group of HSSW samples, relative to the site D, is representative of the hyper-saline waters that are formed in the permanent polynia present between the Drygalski Ice Tongue and Terra Nova Bay. It is characterized by a less pronounced peak of Tb than the ISW, and by a peak of Nd comparable to that of the Tb. Even in this case, we must consider the rocks erosion due to the presence of Drygalski Ice Tongue, this agree also with the high concentration of Nd in the surficial water strongly affected from coast (Nozaki, 2001); in our case it can be assumed the glacier and its catchment area significantly contribute to the specific profile of the water which are formed here.

The ISW, the new-formation waters arising from the interaction of the waters of the Ross Sea with the melt waters of the RIS, appears therefore traceable by the significant high content

of Tb. This peak is yet recognizable even though present with lesser intensity in waters originated by mixing with the ISW namely the LSSW.

Indeed, although data on the REE composition in Pacific Ocean seawater are sparse and scattered, we observed anomalies in the dissolved REE pattern in relation to water masses CDW and AABW present in south Australian Platform and in Kerguelen Plateau. In particular, the data reported by Alibo and Nozaki (Alibo and Nozaki, 2004) relative to the pattern of the REE in samples coming from the Australian southern basin show a significant peak of Tb, especially in deep water, the presence of which could be explained just by mixing with water from the Ross Sea. There is evidence that the inhomogeneous distribution of REE cannot be explained by the systematic trend during scavenging by particulate matter, and must be originated by different external sources to the ocean (Nozaki and Alibo, 2003).

4. Conclusion

REEs data presented here evidence significant differences in the REEs pattern of main water masses present in the Southern Ocean; in particular we can observe some signature in the HSSW, ISW and LSSW. The ISW and HSSW, the principal water masses contributing at the formation of AABW in the Ross Sea area, present significant enrichment in Tb content and for the HSSW also in Nd content. Therefore the dissolved REEs could be used like tracers in the understanding the deep circulation of the Pacific sector of the Southern Ocean.

The characteristic dissolved REEs pattern may derive both from the catchment area of the RIS and the hydrothermal activity of the western area of the Ross Sea.

The Tb anomaly observed in the AABW in the south Australia platform of the Southern Ocean could be explained by the contribution of AABW generated in the Ross Sea region, but also a contribution from other water masses must be hypothesized.

It remains an open question: what is the source area that determines the characteristic profile of the waters of new-formation from the Ross Sea? It is a question to whom can perhaps answer future researches; such investigations should also take into account the areas covered by the Antarctic ice sheet considering the contribution that seems to give the fusion of the Antarctic glaciers and the weathering of rocks under the ice sheets (WAIS and EAIS).

Acknowledgements

References

Abollino, O., Aceto, M., Sacchero, G., Sarzanini, C., Mentasti, E., 1995. Determination of copper, cadmium, iron, manganese, nickel and zinc in Antarctic sea water. Comparison of electrochemical and spectroscopic procedures. Anal Chim Acta 305, 200-206.

Alibo, D.S., Nozaki, Y., 2004. Dissolved rare earth elements in the eastern Indian Ocean: chemical tracers of the water masses. Deep Sea Research Part I: Oceanographic Research Papers 51, 559-576.

Boyer, T.P., Levitus, S., Antonov, J.I., Locarnini, R.A., Garcia, H.E., 2005. Linear trends in salinity for the World Ocean, 1955-1998. Geophys. Res. Lett. 32, L01604.

Bruland, K.W., 1983. Trace Elements in Sea-water. in: Academic, P. (Ed.). Chemical Oceanography. Academic Press, London, pp. 157-220.

Budillon, G., Gremes Cordero, S., Salusti, E., 2002. On the dense water spreading off the Ross Sea shelf (Southern Ocean). Journal of Marine Systems 35, 207-227.

Byrne, R.H., Sholkovitz, E.R., 1996. Marine chemistry and geochemistry of the lanthanides. in: Gschneidner, K.A., Jr., Eyring, L. (Eds.). Handbook on the Physics and Chemistry of Rare Earths Elements. Elsevier, Amsterdam, pp. 497-594.

Capodaglio, G., Coale, K.H., Bruland, K.W., 1990. Lead speciation in surface waters of the eastern North Pacific. Mar Chem 29, 221-233.

Capodaglio, G., Toscano, G., Scarponi, G., Cescon, P., 1989. Lead speciation in the surface waters of the Ross Sea (Antarctica). Annali di Chimica - Rome 79, 543-559.

Capodaglio, G., Turetta, C., Toscano, G., Gambaro, A., Scarponi, G., Cescon, P., 1998. Cadmium, lead and copper complexation in antarctic coastal seawater. Evolution during the austral summer. Int J Environ an Ch 71, 195-226.

Catalano, G., Benedetti, F., Predonzani, S., Goffart, A., Ruffini, S., Rivaro, P., Falconi, C., 2000. Spatial and Temporal Patterns of Nutrient Distributions in the Ross Sea. in: Faranda, F., Guglielmo, L., Ianora, A. (Eds.). Ross Sea Ecology. Springer Berlin Heidelberg, pp. 107-120.

Cincinelli, A., Martellini, T., Bittoni, L., Russo, A., Gambaro, A., Lepri, L., 2008. Natural and anthropogenic hydrocarbons in the water column of the Ross Sea (Antarctica). Journal of Marine Systems 73, 208-220.

Coale, K.H., Michael Gordon, R., Wang, X., 2005. The distribution and behavior of dissolved and particulate iron and zinc in the Ross Sea and Antarctic circumpolar current along 170[deg]W. Deep Sea Research Part I: Oceanographic Research Papers 52, 295-318.

Corami, F., Capodaglio, G., Turetta, C., Soggia, F., Magi, E., Grotti, M., 2005. Summer distribution of trace metals in the western sector of the Ross Sea, Antarctica J Environ Monitor 7 1256-1264.

DeMaster, D.J., Ragueneau, O., Nittrouer, C.A., 1996. Preservation efficiencies and accumulation rates for biogenic silica and organic C, N, and P in high-latitude sediments: The Ross Sea. J. Geophys. Res.-Oceans 101, 18501-18518.

Dinniman, M.S., Klinck, J.M., Smith, Jr., 2003. Cross-shelf exchange in a model of the Ross Sea circulation and biogeochemistry. Deep Sea Research Part II: Topical Studies in Oceanography 50, 3103-3120.

Dubinin, A.V., 2004. Geochemistry of Rare Earth Elements in the Ocean. Lithology and Mineral Resources 39, 289-307.

Fitzwater, S.E., Johnson, K.S., Gordon, R.M., Coale, K.H., Smith, Jr., 2000. Trace metal concentrations in the Ross Sea and their relationship with nutrients and phytoplankton growth. Deep Sea Research Part II: Topical Studies in Oceanography 47, 3159-3179.

Frache, R., Abelmoschi, M.L., Grotti, M., Ianni, C., Magi, E., Soggia, F., Capodaglio, G., Turetta, C., Barbante, C., 2001. Effects of ice melting on particulate Cu, Cd and Pb profiles in Ross Sea waters (Antarctica). Intern.J.Environ.Anal.Chem. 79, 301-313.

Gabrielli, P., Barbante, C., Turetta, C., Marteel, A., Boutron, C., Cozzi, G., Cairns, W., Ferrari, C., Cescon, P., 2006. Direct Determination of Rare Earth Elements at the Subpicogram per Gram Level in Antarctic Ice by ICP-SFMS Using a Desolvation System. Anal Chem 78, 1883-1889.

German, C.R., Masuzawa, T., Greaves, M.J., Elderfield, H., Edmond, J.M., 1995. Dissolved rare earth elements in the Southern Ocean: Cerium oxidation and the influence of hydrography. Geochimica et Cosmochimica Acta 59, 1551-1558.

Goldstein, S.L., Hemming, S.R., 2003. Long lived isotopic tracers in oceanography, paleoceanography, and ice sheet dynamics. Treatise on Geochemistry—The Oceans and Marine Geochemistry. Elsevier, Amsterdam, pp. 453-489.

Gordon, A.L., Orsi, A.H., Muench, R., Huber, B.A., Zambianchi, E., Visbeck, M., 2009. Western Ross Sea continental slope gravity currents. Deep Sea Research Part II: Topical Studies in Oceanography 56, 796-817.

Gordon, L.I., Codispoti, L.A., Jennings, J.C., Jr., Millero, F.J., Morrison, J.M., Sweeney, C., 2000. Seasonal evolution of hydrographic properties in the Ross Sea, Antarctica, 1996-1997. Deep Sea Research Part II: Topical Studies in Oceanography 47, 3095-3117.

Gouretski, V., 1999. The large-scale thermohaline structure of the Ross Gyre. in: Spezie, G., Manzella, G.M.R. (Eds.). Oceanography of the Ross Sea Antarctica. Springer, pp. 77-100.

Gragnani, R., Torcini, S., 1992. Major, minor and trace element distributions in surface water in Terra Nova Bay, Antarctica. Sci Total Environ 125, 289-303.

Grotti, M., Soggia, F., Abelmoschi, M.L., Rivaro, P., Magi, E., Frache, R., 2001. Temporal distribution of trace metals in Antarctic coastal waters. Mar Chem 76, 189-209.

Holland, D.M., Jacobs, S.S., Jenkins, A., 2003. Modelling the ocean circulation beneath the Ross Ice Shelf. Antarctic Science 15, 13-23.

Jacobs, S.S., Giulivi, C.F., 1999. Thermohaline data and ocean circulation on the Ross sea. in: Spezie, G., Manzella, G.M.R. (Eds.). Oceanography of the Ross Sea. Springer-Verlag Italia, Milan, pp. 3-16.

Jacobs, S.S., Giulivi, C.F., Mele, P.A., 2002. Freshening of the Ross Sea During the Late 20th Century. Science 297, 386-389.

Kajiya, T., Aihara, M., Hirata, S., 2004. Determination of rare earth elements in seawater by inductively coupled plasma mass spectrometry with on-line column pre-concentration using 8-quinolinole-immobilized fluorinated metal alkoxide glass. Spectrochimica Acta Part B: Atomic Spectroscopy 59, 543-550.

Karner, G.D., Studinger, M., Bell, R.E., 2005. Gravity anomalies of sedimentary basins and their mechanical implications: Application to the Ross Sea basins, West Antarctica. Earth Planet Sc Lett 235, 577-596.

Lawrence, M.G., Kamber, B.S., 2007. Rare Earth Element Concentrations in the Natural Water Reference Materials (NRCC) NASS-5, CASS-4 and SLEW-3. Geostandards and Geoanalytical Research 31 95-103.

Lerche, D., Nozaki, Y., 1998. Rare earth elements of sinking particulate matter in the Japan Trench. Earth Planet Sc Lett 159, 71-86.

Mantyla, A.W., Reid, J.L., 1995. On the origins of deep and bottom waters of the Indian Ocean. Journal of Geophysical Research 100, 2417-2439.

Nozaki, Y., 2001. Rare Earth Elements and their Isotopes in the Ocean. in: Steele, J., H. (Ed.). Encyclopedia of Ocean Sciences. Academic Press, Oxford, pp. 2354-2366.

Nozaki, Y., Alibo, D.-S., 2003. Dissolved rare earth elements in the Southern Ocean, southwest of Australia: Unique patterns compared to the South Atlantic data. Geochemical Journal 37 47-62.

Orsi, A.H., Johnson, G.C., Bullister, J.L., 1999. Circulation, mixing, and production of Antarctic Bottom Water. Progress In Oceanography 43, 55-109.

Orsi, A.H., Wiederwohl, C.L., 2009. A recount of Ross Sea waters. Deep Sea Research Part II: Topical Studies in Oceanography 56, 778-795.

Piepgras, D.J., Jacobsen, S.B., 1992. The behavior of rare earth elements in seawater: Precise determination of variations in the North Pacific water column. Geochimica et Cosmochimica Acta 56, 1851-1862.

Rivaro, P., Ianni, C., Massolo, S., Abelmoschi, M.L., De Vittor, C., Frache, R., 2011. Distribution of dissolved labile and particulate iron and copper in Terra Nova Bay polynya (Ross Sea, Antarctica) surface waters in relation to nutrients and phytoplankton growth. Continental Shelf Research 31, 879-889.

Scarponi, G., Capodaglio, G., Toscano, G., Barbante, C., Cescon, P., 1995. Speciation of Lead and Cadmium in Antarctic Seawater: Comparison with Areas Subject to Different Anthropic Influence. Microchem J 51, 214-230.

Scarponi, G., Capodaglio, G., Turetta, C., Barbante, C., Cecchini, M., Toscano, G., Cescon, P., 1997. Evolution of cadmium and lead contents in antarctic coastal seawater during the austral summer. Int J Environ an Ch 66, 23-49.

Sholkovitz, E.R., Elderfield, H., Szymczak, R., Casey, K., 1999. Island weathering: river sources of rare earth elements to the Western Pacific Ocean. Mar Chem 68, 39-57.

The Wissard Science Team, 2012. WISSARD McMurdo Ice Shelf Test Field Report. http://www.wissard.org/sites/default/files/reports/wissard-mis-test-report-summary.pdf.

Thompson, M., Ellison, S.L., Wood, R., 2002. Harmonized guidelines for single-laboratory validation of methods of analysis (IUPAC Technical Report). Pure and Applied Chemistry 74, 835-855.

Turetta, C., Barbante, C., Capodaglio, G., Gambaro, A., Cescon, P., 2010. The distribution of dissolved thallium in the different water masses of the western sector of the Ross Sea (Antarctica) during the austral summer. Microchem J 96, 194-202.

Turetta, C., Cozzi, G., Barbante, C., Capodaglio, G., Cescon, P., 2004. Trace elements determination in seawater by ICP-SFMS coupled with a micro-flow nebulization/desolvation. Anal Bioanal Chem 380, 258-268.

Willie, S.N., Sturgeon, R.E., 2001. Determination of transition and rare earth elements in seawater by flow injection inductively coupled plasma time-of-flight mass spectrometry. Spectrochimica Acta Part B: Atomic Spectroscopy 56, 1707-1716.

Winter, B.L., Johnson, C.M., Clark, D.L., 1997. Strontium, neodymium, and lead isotope variations of authigenic and silicate sediment components from the Late Cenozoic Arctic Ocean:

Implications for sediment provenance and the source of trace metals in seawater. Geochimica et Cosmochimica Acta 61, 4181-4200.

Zhang, Y., Lacan, F., Jeandel, C., 2008. Dissolved rare earth elements tracing lithogenic inputs over the Kerguelen Plateau (Southern Ocean). Deep Sea Research Part II: Topical Studies in Oceanography 55, 638-652.
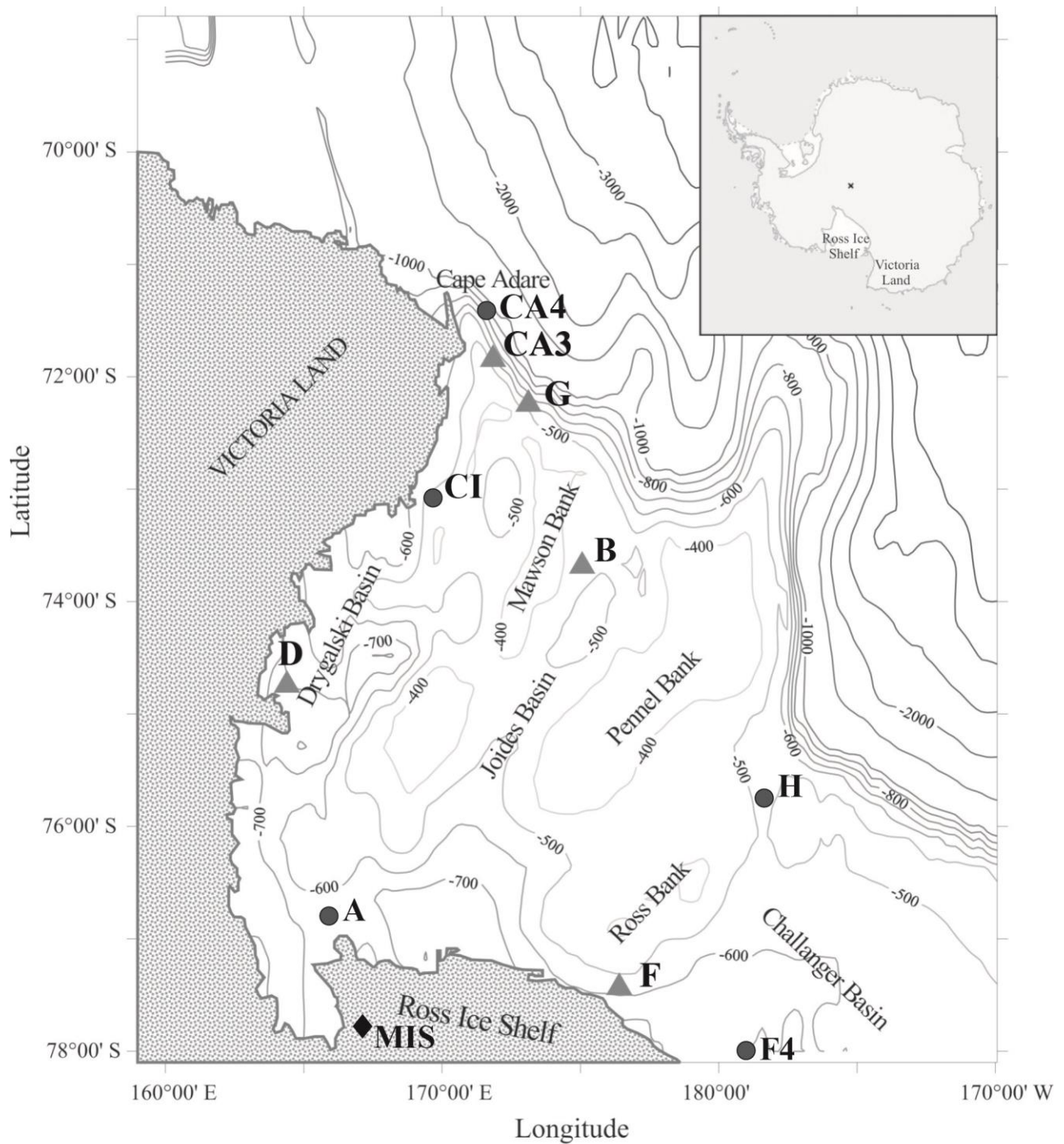
Figure 1. Sampling sites; simplified map of the western sector of the Ross sea (bottom topography in meters). Triangles represent the 2002e2003 campaign; dots represent the 2005e2006 campaign; diamonds represent the boreholes of the Wissard project samples (Turetta et al., 2010, modified). Each depth profile is indicated as a single point..
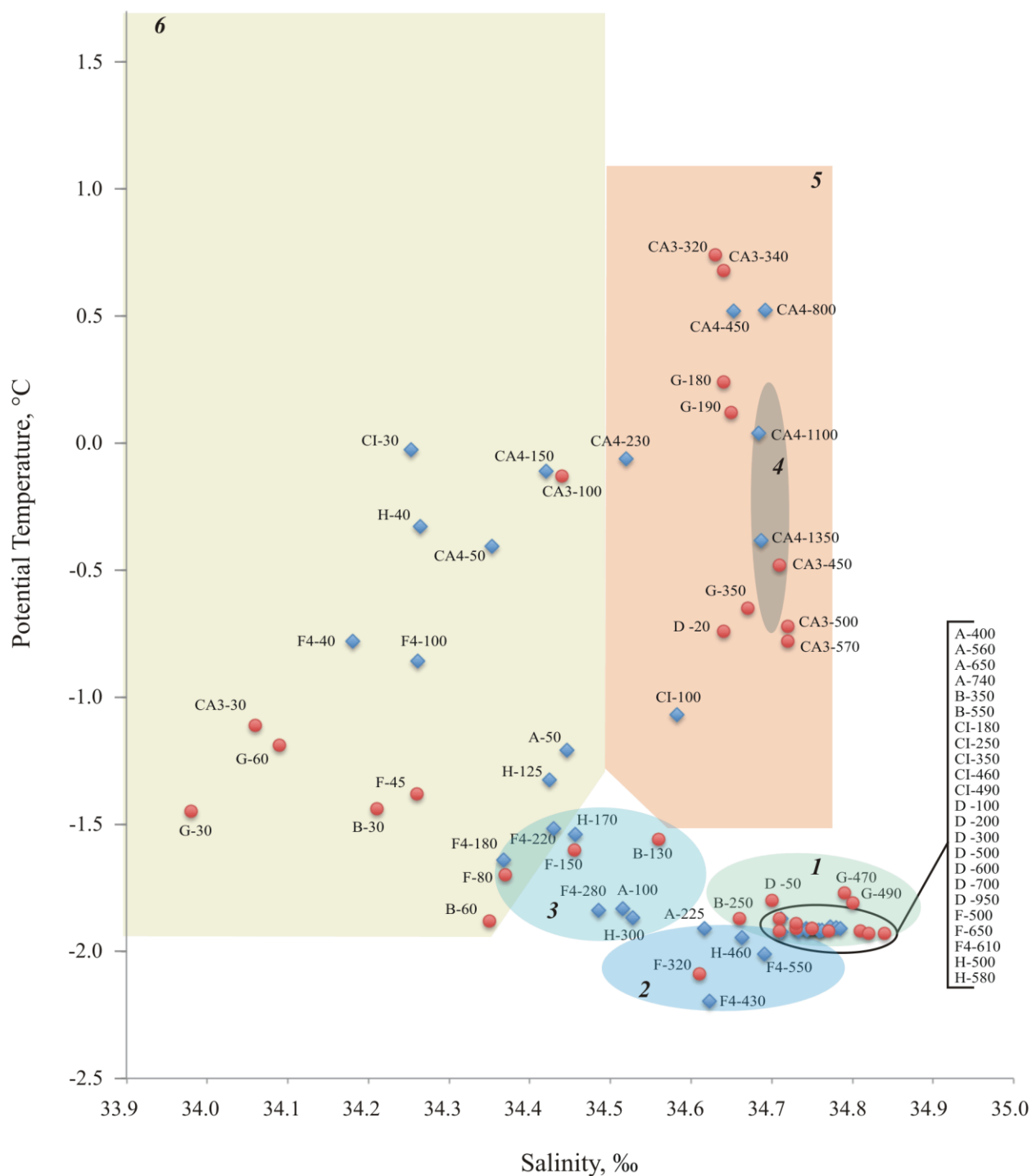
Figure 2. Distribution of samples in terms Potential Temperature vs. Salinity (q-S) space. Shaded areas from 1 to 6 represent HSSW, ISW, LSSW, AABW, MCDW and AASW domains. Samples in overlapping areas are of uncertain attribution. Dots and diamonds represent the samples from the 2002e2003 and 2005e2006 sampling campaign, respectively.
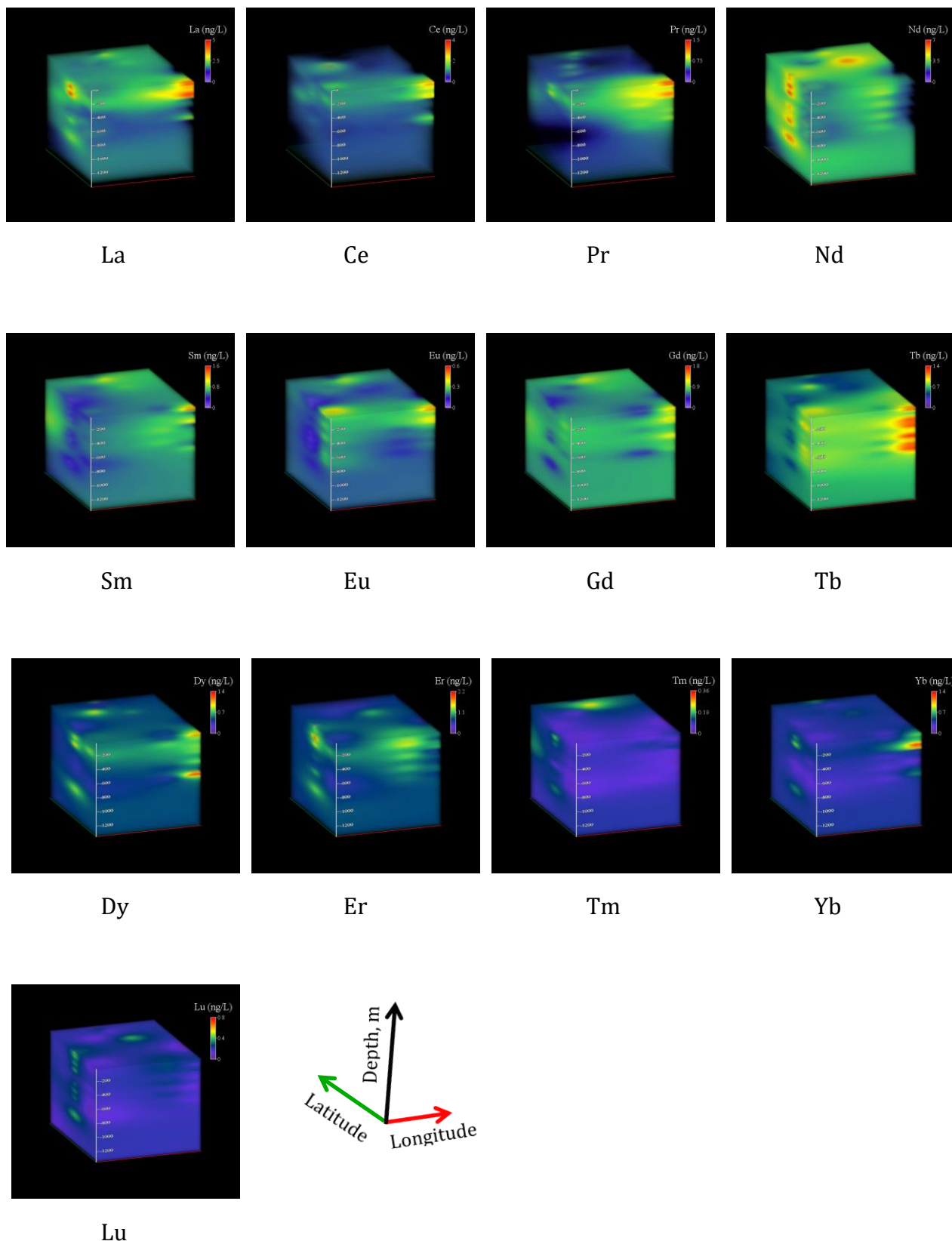
Figure 3. 3D REE distribution along vertical profiles in the Ross Sea. The depth axis is from 0 to 1350 m; the latitude axis is from 71 32.320 S to 77 56.340 S; the longitude axis is from 164 28.000 E to 177 23.110 W. In the colour scale, blue/purple represents the lower concentration values, while red represents higher concentration values. Concentrations are indicated in ng L1 . (For interpretation of the references to colour in this figure legend, the reader is referred to the web version of this article.).
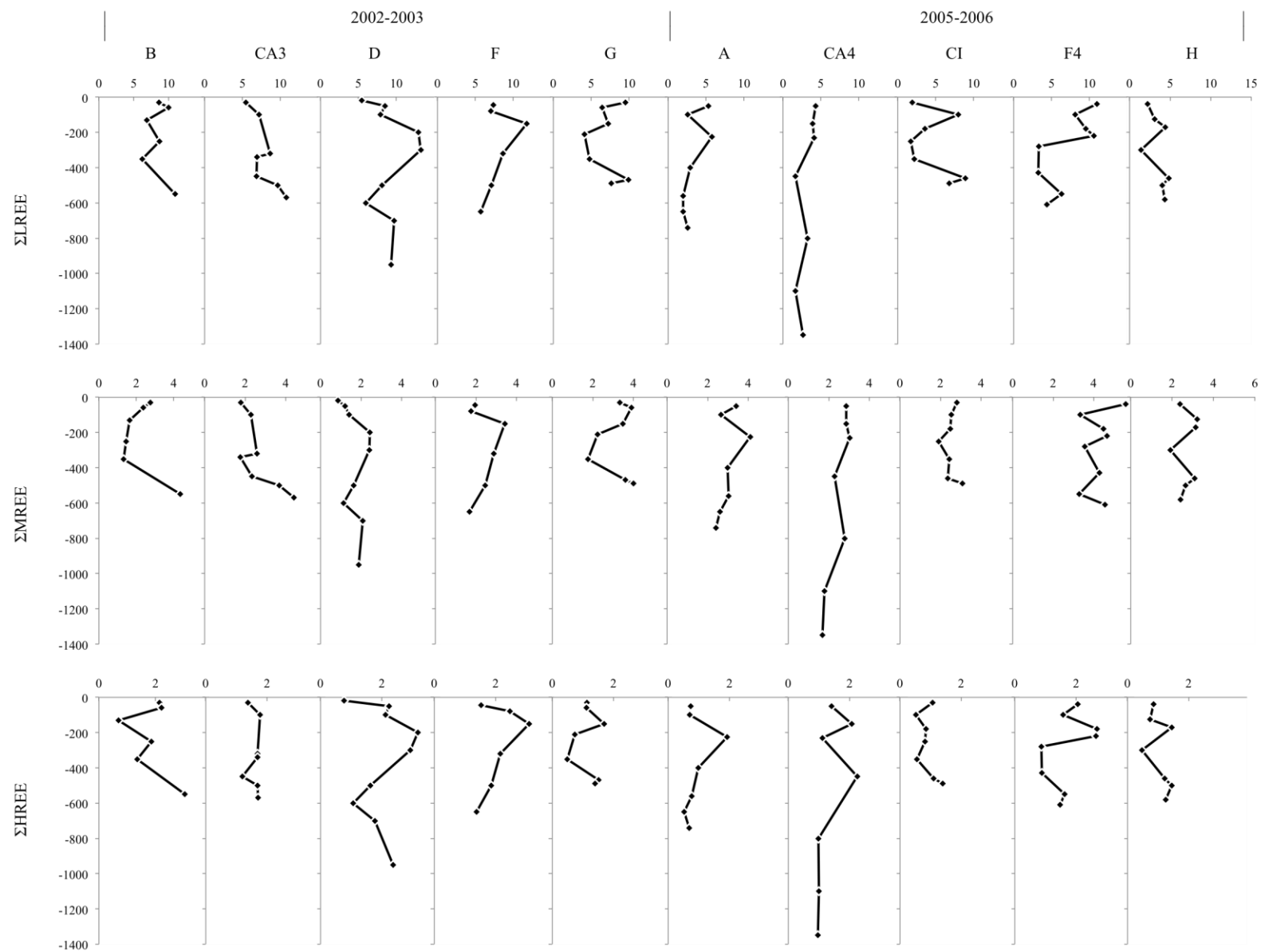
Figure 4. Vertical distribution of SLREE, SMREE, and SHREE for depth profiles. Concentrations are indicated in ng L^{-1} .
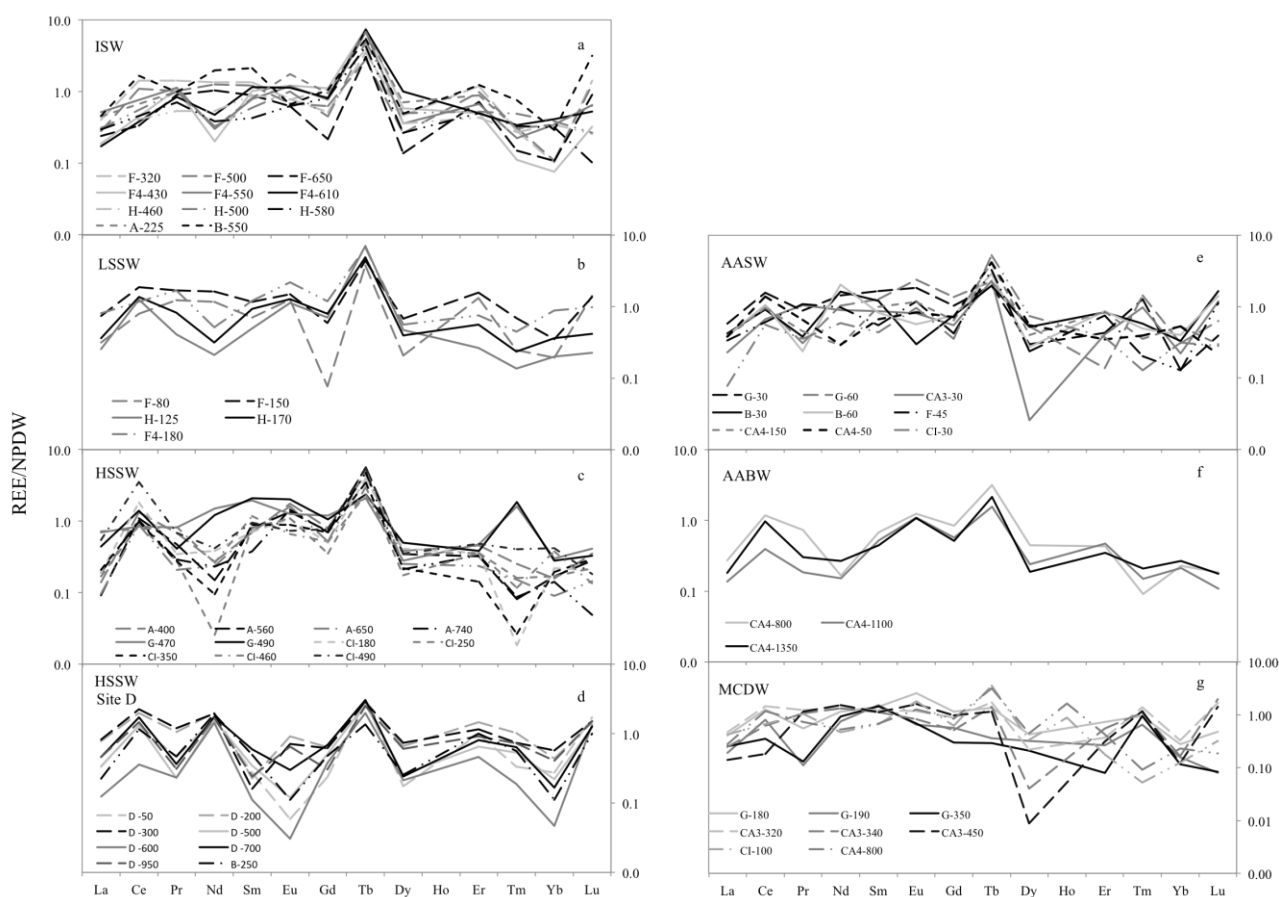
Figure 5. The pattern of dissolved REEs/PAAS in the new-formation water masses of the Ross sea (dotted lines represent 2002-2003 campaign; continuous lines represent 2005-2006 campaign).
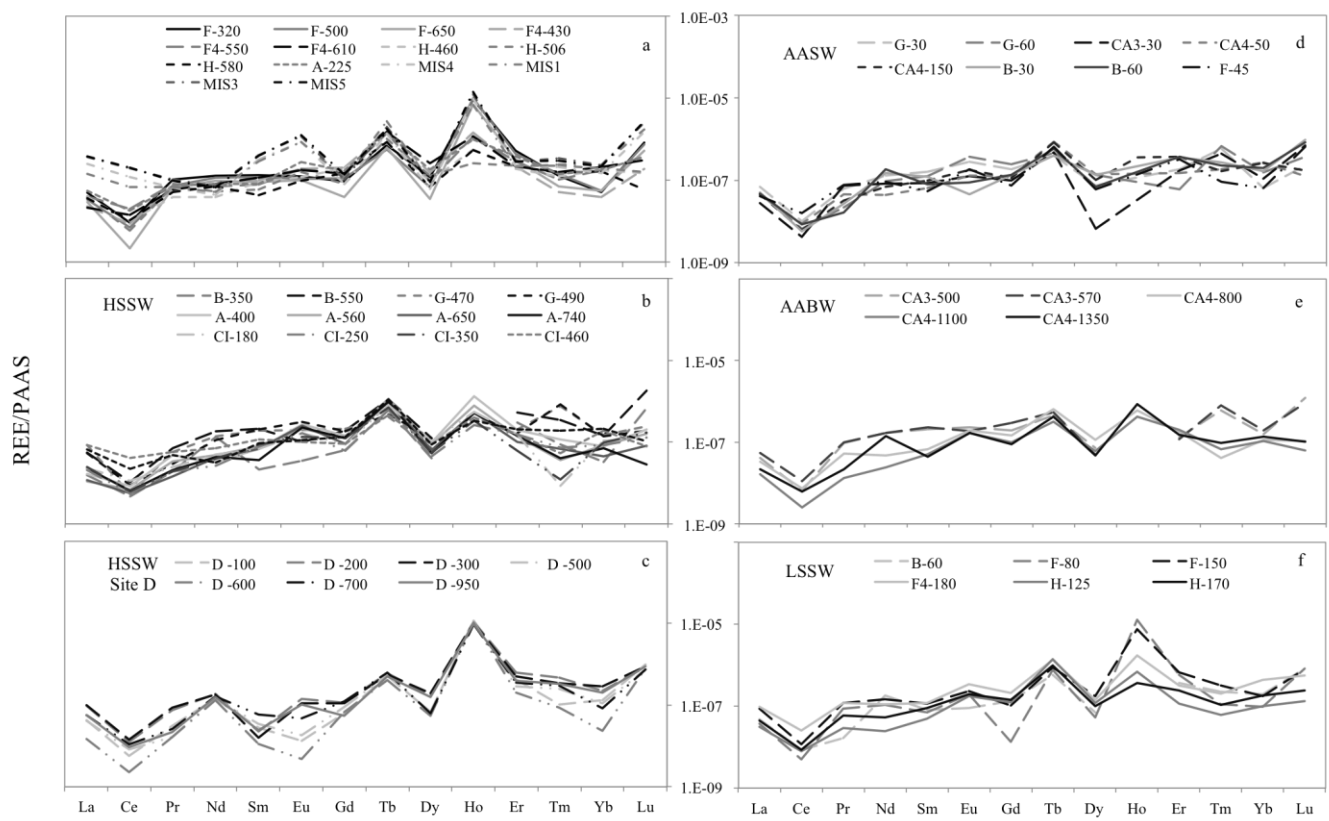
Figure 6. Pattern of dissolved REEs/PAAS in the newly formed water masses of the Ross Sea.
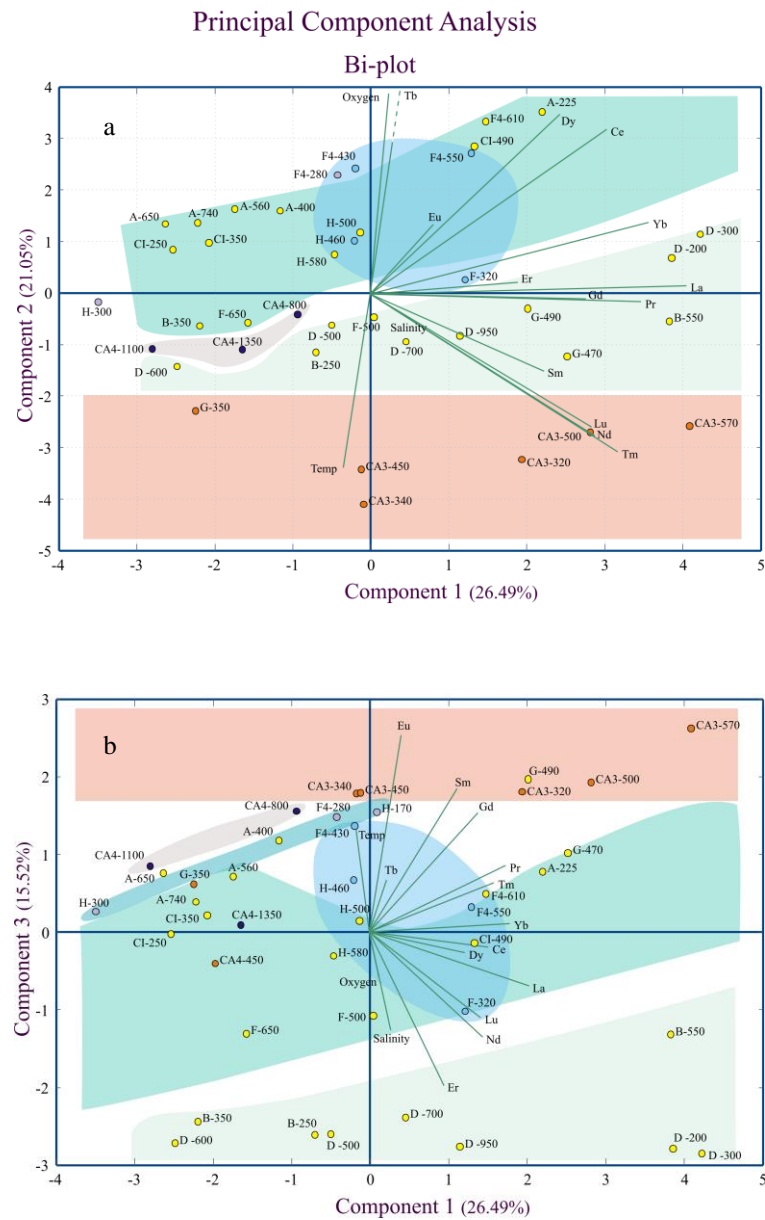
Figure 7. Graphs of Principal Component Analysis performed on samples deeper than 200 m. Bi-plots of first vs. second component (a) and first vs. third component (b)

Table 1: Geographical coordinates of profiles. Depth column indicates the floor depth.

Profile	Latitude S	Longitude E/W	Depth (m)
2002-2003			
B	74°01.10' S	175°04.60' E	581
CA3	71°56.00' S	171°52.00'E	630
D	75° 07.00' S	164° 28.00' E	1050
F	77°32.30' S	176°02.00' E	700
G	72°20.00'S	173°03.00' E	510
2005-2006			
A	76°41.00' S	169°04.00' E	790
CA4	71°32.32' S	172°17.16' E	1688
CI	73°13.58' S	171° 13,44' E	537
F4	77°56.34' S	177°53.09' W	654
H	75°57.06' S	177°23.11' W	615

Table 2: Literature data for REEs in NASS-5; standard deviation value in brackets. Mean values for REEs measured in blank solutions; standard deviation value in brackets.

	La (ng L⁻¹)	Ce (ng L⁻¹)	Pr (ng L⁻¹)	Nd (ng L⁻¹)	Sm (ng L⁻¹)	Eu (ng L⁻¹)	Gd (ng L⁻¹)	Tb (ng L⁻¹)	Dy (ng L⁻¹)	Ho (ng L⁻¹)	Er (ng L⁻¹)	Tm (ng L⁻¹)	Yb (ng L⁻¹)	Lu (ng L⁻¹)
NASS-5														
(Willie and Sturgeon, 2001)	12.8 (1.2)	4.0 (0.6)	1.5 (0.2)	9.9 (1.8)	4.0 (0.4)	0.24 (0.05)	1.53 (0.28)	0.29 (0.05)	1.65 (0.28)	0.36 (0.05)	1.24 (0.24)	0.15 (0.03)	1.10 (0.24)	0.20 (0.04)
(Shaw et al., 2003)	12.1 (0.5)	4.5 (0.7)	2.0 (0.2)	8.9 (0.5)	4.5 (0.2)	0.27 (0.03)	1.6 (0.08)	0.21 (0.04)	1.78 (0.07)	0.37 (0.04)	1.37 (0.03)	0.15 (0.03)	1.2 (0.04)	0.18 (0.02)
(Lawrence and Kamber, 2007)	12.19 (1.14)	5.72 (0.69)	2.09 (0.19)	8.43 (0.65)	4.74 (0.34)	0.33 (0.03)	1.83 (0.15)	0.27 (0.03)	1.82 (0.20)	0.47 (0.06)	1.43 (0.20)	0.21 (0.04)	1.29 (0.38)	0.19 (0.06)
Max-Planck-Institute database – GeoReM	12.1 (0.22)	2.02 (0.19)	0.98 (0.07)	3.39 (0.2)	3.41 (0.9)	0.41 (0.08)	1.03 (0.07)	0.5 (0.02)	0.95 (0.8)	0.51 (0.01)	0.75 (0.03)	0.41 (0.05)	1.33 (0.03)	0.49 (0.04)
This work	12.5 (0.38)	4.9 (0.43)	2.1 (0.26)	9.0 (0.39)	4.0 (0.37)	0.31 (0.07)	1.6 (0.10)	0.31 (0.07)	1.7 (0.14)	0.48 (0.03)	1.4 (0.14)	0.21 (0.03)	1.26 (0.04)	0.20 (0.02)
Blank (Mean of 10 measures)	0.24 (0.027)	0.19 (0.005)	0.024 (0.005)	0.36 (0.04)	0.43 (0.014)	0.12 (0.005)	0.46 (0.04)	0.05 (0.006)	0.036 (0.007)	0.009 (0.001)	0.035 (0.009)	0.018 (0.003)	0.05 (0.01)	0.026 (0.004)

Table 3: Mean, minimum and maximum values for measured REEs in samples (for sampling site see figure 1).

	La (ng L⁻¹)	Ce (ng L⁻¹)	Pr (ng L⁻¹)	Nd (ng L⁻¹)	Sm (ng L⁻¹)	Eu (ng L⁻¹)	Gd (ng L⁻¹)	Tb (ng L⁻¹)	Dy (ng L⁻¹)	Ho (ng L⁻¹)	Er (ng L⁻¹)	Tm (ng L⁻¹)	Yb (ng L⁻¹)	Lu (ng L⁻¹)
Mean	1.87	0.81	0.52	3.67	0.62	0.21	0.74	0.66	0.50	3.60	0.775	0.10	0.40	0.20
Min	0.33	0.10	0.05	0.91	0.03	0.01	0.053	0.052	0.01	0.27	0.105	0.004	0.07	0.012
Max	4.61	3.01	1.34	6.94	1.61	0.53	1.818	1.367	1.37	13.66	2.119	0.38	1.33	0.81

Table 4a. values for Σ LREE, Σ MREE, Σ HREE, La/Yb and Gd/Yb PAAS normalized ratio for 2002-2003 sampling campaign.

	Depth	ΣLREE (La-Nd)	ΣMREE (Sm-Dy)	ΣHREE (Er-Lu)	La/Yb	Gd/Yb
	m	ng L^{-1}				
02-03						
B-30	-30	8.60	2.75	2.14	0.31	0.81
B-60	-60	9.97	2.37	2.21	0.24	0.67
B-130	-130	6.90	1.64	0.69	0.82	1.72
B-250	-250	8.69	1.46	1.86	0.49	1.52
B-350	-350	6.22	1.33	1.35	0.47	1.96
B-550	-550	10.90	4.35	3.04	0.38	1.30
CA3-30	-30	5.44	1.78	1.38	0.25	0.88
CA3-100	-100	7.18	2.30	1.78	0.33	0.95
CA3-320	-320	8.63	2.60	1.69	0.34	0.95
CA3-340	-340	6.90	1.77	1.70	0.35	1.08
CA3-450	-450	6.83	2.32	1.20	0.27	2.85
CA3-500	-500	9.64	3.68	1.70	0.26	1.23
CA3-570	-570	10.78	4.41	1.71	0.28	1.57
D-20	-20	5.41	0.87	0.77	1.30	2.39
D-50	-50	8.53	1.22	2.24	0.29	0.30
D-100	-100	7.93	1.40	2.13	0.33	0.49
D-200	-200	12.89	2.44	3.18	0.43	0.51
D-300	-300	13.22	2.41	2.93	0.35	0.38
D-500	-500	8.10	1.63	1.63	0.37	0.81
D-600	-600	5.99	1.13	1.06	0.63	2.86
D-700	-700	9.68	2.08	1.78	0.66	1.47
D-950	-950	9.34	1.88	2.37	0.28	0.27
F-45	-45	7.36	1.96	1.52	0.63	1.16
F-80	-80	7.02	1.76	2.47	0.39	0.14
F-150	-150	11.80	3.42	3.09	0.51	0.60

F-320	-320	8.62	2.89	2.16	0.95	1.81
F-500	-500	7.13	2.47	1.86	0.62	2.04
F-650	-650	5.69	1.69	1.38	0.54	0.71
G-30	-30	9.52	3.32	1.13	1.06	2.79
G-60	-60	6.41	3.91	1.11	0.30	1.54
G-180	-150	7.21	3.47	1.69	0.36	1.46
G-190	-210	4.08	2.25	0.74	0.29	1.27
G-350	-350	4.76	1.77	0.49	0.52	0.92
G-470	-470	9.91	3.60	1.52	0.56	1.43
G-490	-490	7.63	4.01	1.40	0.38	1.33

Table 4b. Values for Σ LREE, Σ MREE, Σ HREE, La/Yb and Gd/Yb PAAS normalized ratio for 2005-2006 sampling campaign and WISSARD sample (MIS mean value).

	Depth	ΣLREE (La-Nd)	ΣMREE (Sm-Dy)	ΣHREE (Er-Lu)	La/Yb	Gd/Yb
	m	ng L⁻¹				
05-06						
A-50	-50	5.27	3.42	0.73	0.80	2.11
A-100	-100	2.60	2.65	0.70	0.17	1.41
A-225	-225	5.76	4.10	1.93	0.31	0.98
A-400	-400	2.90	3.00	0.99	0.21	1.81
A-560	-560	1.94	3.04	0.77	0.13	1.50
A-650	-650	1.97	2.60	0.52	0.26	2.02
A-740	-740	2.60	2.41	0.68	0.33	1.74
CA4-50	-50	4.31	2.87	1.41	0.17	0.47
CA4-150	-150	3.89	2.86	2.07	0.17	0.43
CA4-230	-230	4.11	3.03	1.11	0.33	0.07
CA4-450	-450	1.64	2.29	2.25	0.30	4.95
CA4-800	-800	3.22	2.78	0.98	0.29	1.29
CA4-1100	-1100	1.62	1.78	1.00	0.15	0.95
CA4-1350	-1350	2.67	1.70	0.96	0.16	0.68
CI-30	-30	1.88	2.80	1.07	0.06	0.40
CI-100	-100	7.96	2.54	0.52	0.81	1.74
CI-180	-180	3.60	2.48	0.86	0.21	0.80
CI-250	-250	1.68	1.90	0.82	0.24	0.73
CI-350	-350	2.18	2.43	0.56	0.26	1.27
CI-460	-460	8.94	2.36	1.10	0.46	0.49
CI-490	-490	6.78	3.08	1.40	0.31	0.65
F4-40	-40	10.96	5.59	2.05	0.38	0.82
F4-100	-100	8.14	3.34	1.57	0.36	0.79
F4-180	-180	9.52	4.48	2.68	0.22	0.48

F4-220	-220	10.59	4.65	2.64	0.26	0.45
F4-280	-280	3.29	3.57	0.87	0.26	1.24
F4-430	-430	3.21	4.27	0.88	0.59	5.18
F4-550	-550	6.33	3.29	1.63	0.35	0.78
F4-610	-610	4.39	4.55	1.49	0.10	0.71
H-40	-40	2.22	2.39	0.85	0.18	0.65
H-125	-125	3.10	3.22	0.74	0.31	1.26
H-170	-170	4.40	3.14	1.44	0.24	0.78
H-300	-300	1.43	1.91	0.46	0.44	2.00
H-460	-460	4.81	3.09	1.22	0.22	1.10
H-500	-500	4.01	2.65	1.44	0.19	0.41
H-580	-580	4.32	2.40	1.24	0.22	0.90
MIS	-870	12.90	6.54	4.64	0.61	0.49